Current Optics and Photonics
Vol. 4, No. 6, December 2020, pp. 477-482

ISSN: 2508-7266(Print) / ISSN: 2508-7274(Online)
DOI: https://doi.org/10.3807/COPP.2020.4.6.477

Spectral-shape-controllable Chirped Fiber Bragg Grating with a Photomechanical Microactuator: Simulation and Experiment

Jong-Ju Moon, Youngmin Ko, Su-Jeong Park, and Tae-Jung Ahn*

Department of Photonic Engineering, Chosun University, Gwangju 61452, Korea

(Received August 15, 2020 : revised October 19, 2020 : accepted October 28, 2020)

Recently, one of the authors has been reported an optically tunable fiber Bragg grating (FBG) with a photomechanical polymer. It was based on a typical FBG with a downsized diameter of 60 μm, coated with azobenzene-containing polymer material. Azobenzene is a well-known reversibly photomechanical stretchable material under ultraviolet (UV) light. The small part of the functional-coating region on the FBG absorbed UV light, which pulled the UV-exposed part of the grating. It was selectable as tunable FBG or tunable chirped FBG, by adjusting the position of UV exposure on the grating. As proof of concept for the tunable FBG device, the characteristics just including UV-induced center-wavelength shift and spectral-width changes of the device were reported. In this paper, we report for the first time that the microactuator makes it possible to control the spectral shape of the FBG reflection, according to the specifications (shape and intensity) of the UV beam that reaches the FBG coated with the azobenzene polymer. In addition, we provide the group-delay profiles for the chirped FBG, so that the sign of its dispersion (normal or anomalous) can be tailored by simply selecting the moving direction of the UV light's displacement in the experiment.

Keywords : Ultraviolet, Chirped fiber Bragg grating, Tunable device
OCIS codes : (060.2340) Fiber optics components; (060.3735) Fiber Bragg gratings; (160.5470) Polymers

I. INTRODUCTION

Undoubtedly, fiber Bragg gratings (FBGs) have a long history and are important optical devices that continue to be used in various research fields, such as optical communication, optical sensors, optical filters, pulse shaping, and optical fiber lasers [1, 2]. The FBG is a passive device and generally has the function of selecting wavelengths within a typical spectral width of 0.5 nm. Chirped FBGs (CFBGs), in which the grating period increases linearly, are also used in various fields such as dispersion compensation devices, optical time-delay lines, optical filters, optical sensors and pulse-shaping devices [3, 4].

Several studies have been carried out to develop passive optical-fiber gratings and chirped optical-fiber gratings as active devices capable of changing wavelength and spectral width [5-8]. We have recently proposed an optically tunable FBG that can be reconfigured to provide either a wavelength-tunable FBG or a tunable CFBG, involving a fiber-grating device in combination with a UV-lighting system [9]. The tunable FBG was prepared by uniformly coating it with a functional polymer and using optically controllable microactuators on the FBG. The structure of the polymer material could be reversibly changed by absorbing UV light, which induced stretching of the polymer coating on the FBG and a corresponding wavelength shift in the FBG's resonance. The variation in the grating's spacing was determined by the amount of UV intensity at each position of the FBG. The UV-exposed azobenzene material behaved like a microactuator that could optionally pull a small part of the fiber-grating device. A tunable FBG, the wavelength of which was shifted linearly with a constant spectral width, was implemented by irradiating the FBG with a uniform UV intensity. A tunable CFBG was also implemented, by irradiating the FBG with a nonuniform

*Corresponding author: taejung.ahn@chosun.ac.kr, ORCID 0000-0001-8801-9846
Color versions of one or more of the figures in this paper are available online.

UV intensity along its length.

In the paper we provide simulation and experimental results for the spectral shaping of the reflection spectra from CFBGs with different UV-intensity profiles, complementing the set of results reported in our previous paper [9]. A UV LED with a Gaussian-like intensity profile is normally used as a UV-light source. We anticipate that the spectral shape of CFBG reflection can be controlled by shaping the UV beam. The UV-beam profile that illuminates the FBG is tailored by modifying the alignment of the UV LED with respect to the FBG, as well as the intensity of the UV light. Also, a group-delay profile (*i.e.* dispersion) can be produced and tuned through tailoring the intensity gradient of the UV light on the FBG. We report for the first time experimental measurements of the group-delay profiles of CFBGs with different UV intensity gradients, and we confirm how the system allows us to tune the value and sign of the resulting dispersion, from normal to anomalous dispersion. Dispersion values of +27.6 ps/nm and -25.68 ps/nm were measured using opposite UV-intensity gradients. Through the produced grating-period chirping process, the width of the FBG's spectral response was increased to approximately 2 nm, from the spectral width of 0.15 nm for a typical uniform FBG.

II. THEORY

Azobenzene undergoes photoisomerization of *trans* and *cis* isomers; *cis*-azobenzene relaxes back to its *trans isomer*. The two isomers can be switched with ultraviolet light, which corresponds to the energy gap of the π-π^* (S_2 state) transition for *trans*-to-*cis* conversion, and visible light, which matches that of the n-π^* (S_1 state) transition for *cis*-to-*trans* isomerization. For a variety of reasons, the *cis* isomer is less stable than the *trans* [10]. The photo-isomerization of azobenzene is a form of light-induced molecular motion. This isomerization can also lead to motion on larger length scales. The photoisomerization reaction has been applied to various applications, such as microactuators, microrobotics, photoinduced shape-memory polymer, and UV sensors [11]. Here we thought that azobenzene could be used as an optically controllable microactuator to locally change the grating spacing of an azobenzene-coated FBG region exposed by UV light.

We calculated the reflection spectra of CFBGs with UV-induced grating-spacing profiles, considering nonuniform FBGs formed within the core of an optical fiber with an average refractive index n_0. The refractive-index profile of a CFBG can be expressed as [1]

$$n = n_0 + \Delta n \cos\{\phi(z)\}, \tag{1}$$

where Δn represents the constant amplitude of the refractive-index perturbation along z, and the spatial frequency of $2\pi/(\Lambda(z))$ represents the derivative of $\phi(z)$ as a function of z. $\Lambda(z)$ denotes the grating spacing as function of z, which is the distance along the FBG's longitudinal axis, determined by the optically controllable microactuator. Here we assume no slowly varying envelope in the index perturbation, such that there is no refractive-index apodization; however, a variation of the grating spacing $\Lambda(z)$ along the azobenzene-coated CFBG length is induced through UV irradiation. Thus the grating spacing along the FBG is, in fact, determined by the intensity distribution of the UV light along the grating's length. The Bragg wavelength λ_B is related to the effective grating index n_{eff} as $\lambda_B = 2n_{eff}\Lambda(z)$. Using coupled-mode theory, the reflection spectrum of the FBG is given by [1]

$$R(\lambda) = \frac{\kappa^2 \sinh^2(sL)}{s^2 \cosh^2(sL) - \delta^2}, \tag{2}$$

where $R(\lambda)$ represents the reflectivity as a function of wavelength λ and the grating length is L. κ denotes the absolute value of the coupling coefficient, given by

$$\kappa = \frac{\eta \pi \Delta n}{\lambda}, \tag{3}$$

where η is defined as the fraction of the fiber mode power contained within the fiber core, which is here assumed to be unity. δ represents the detuning from the Bragg wavelength, as expressed by

$$\delta = \beta - \frac{\pi}{\Lambda(z)} = \frac{2\pi}{\lambda} n_{eff} - \frac{\pi}{\Lambda(z)}, \tag{4}$$

where β is the propagation constant of the fundamental mode propagating along the FBG, and $s^2 = \kappa^2 - \delta^2$. When the UV LED produces a Gaussian-shaped UV beam, the grating spacing is dominantly varied by local elongation of the grating with the microactuator, as illustrated in Fig. 1. Here UV-induced index change of the FBG is negligible, because the most of the UV intensity is absorbed in the azobenzene polymer. The UV-induced chirped grating spacing along the fiber length is expressed by

$$\Lambda(z) = \Lambda_0 + \Delta\Lambda \exp\left\{\frac{-(z - L/2)^2}{L^2}\right\}, \tag{5}$$

where Λ_0 is the initial grating spacing at the beginning of the grating and $\Delta\Lambda$ is an increment factor of the grating spacing. Thus the grating spacing is assumed to follow a Gaussian profile as a function of the fiber's length.

The grating spacing $\Lambda(z)$ is apodized according to the Gaussian distribution profile of the UV light when the center of the LED is placed precisely at the grating's center (Fig. 1). A chirped FBG can be obtained by shifting the center of the UV illumination with respect to the location of the FBG [9]. Then the FBG is placed on a tail of the Gaussian profile, which provides a gradually varied grating

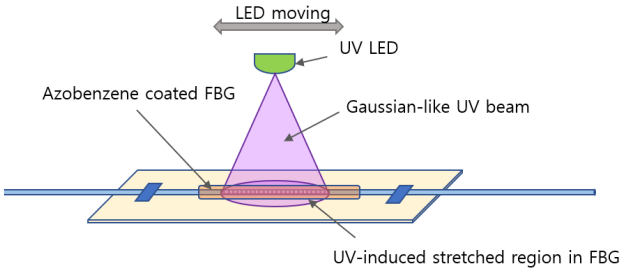

FIG. 1. Spectral-shape-controllable CFBG, based on photo-mechanical azobenzene polymer and a UV LED.

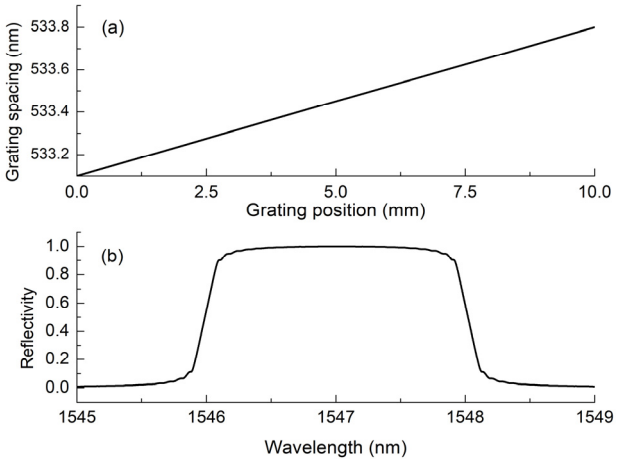

FIG. 2. Linearly chirped FBG profile: (a) linearly chirped grating spacing along the FBG, and (b) reflection spectrum of the CFBG.

spacing in the CFBG. If the UV-induced chirped grating period is perfectly linear, as in Fig. 2(a), then the flat-top reflection spectrum of the CFBG is calculated by Eq. (4), as shown in Fig. 2(b). The bandwidth of the spectrum is related to the slope of the grating-spacing function $\Lambda(z)$. n_0 and Δn were set to 1.45 and 5×10^{-5} respectively. However, the tail of the Gaussian distribution profile is *not* linear. When the UV LED is moved toward one side of the FBG, a UV-induced nonlinear grating-spacing profile is obtained, as presented in Fig. 3(a). Before the FBG center, Fig. 3(a) shows a linear characteristic, but beyond the center it shows a nonlinear characteristic. The grating period up to a position of 7 mm is likely to be a linear function, which induces the flat-top shape of the reflection spectrum from 1546 nm to 1547.5 nm in Fig. 3(b), while the nonlinear curve of the grating profile beyond 7 mm induces a shark-fin-like spectrum. This is the reason why the longer-wavelength components in the region of 1546.5-1548 nm are fully reflected beyond the FBG position of 7 mm.

On the contrary, the beginning of the FBG may follow a nonlinear grating spacing profile, with the grating spacing being consequently and gradually linearly chirped along the FBG, as shown in Fig. 4(a). In this case we can imagine

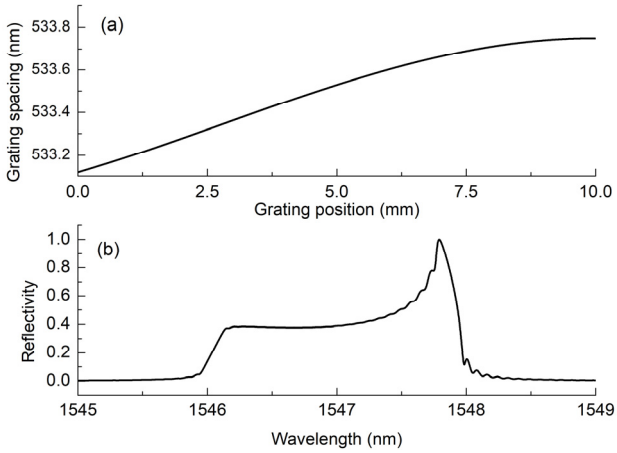

FIG. 3. Nonlinearly chirped FBG profile, having a more nonlinear grating-spacing change after the center of the FBG: (a) nonlinearly chirped grating spacing along the FBG, and (b) reflection spectrum of the CFBG.

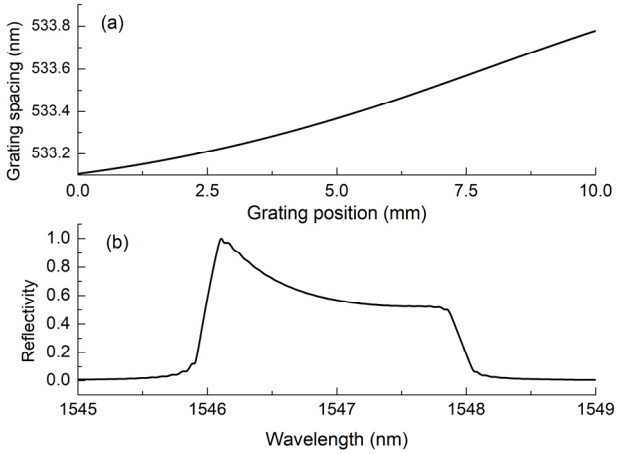

FIG. 4. Nonlinearly chirped FBG profile, having more nonlinear grating-spacing change before the FBG center: (a) nonlinearly chirped grating spacing along the FBG, and (b) reflection spectrum of the CFBG.

that the center of the UV LED is moved a bit to the right from the grating profile of Fig. 3(a). Figure 4(b) shows the asymmetric reflection spectrum of the CFBG enabled by the grating profile of Fig. 4(a). The spectral shape is opposite that in Fig. 3(b), as this depends on whether the nonlinear curve of the grating profile is at the beginning or the end of the FBG.

We found that the UV-induced chirped grating spacing of the azobenzene-coated FBG provides various spectral shapes related to the UV-intensity distribution. We can control the shape of the UV-intensity profile exposed on the azobenzene-coated FBG by means of the height of the UV LED above the FBG, the voltage applied to the UV LED, and the offset alignment of the LED from the FBG. For proof of concept, we have demonstrated the shape-controlled reflection spectra of a CFBG in experiments.

III. EXPERIMENTS AND RESULTS

For the optically tunable CFBG we use an etched FBG, to improve the applied-strain sensitivity of the grating. The strain sensitivity of the grating is inversely proportional to the square of its diameter [12]. When an etched FBG with a diameter of 60 μm is used, it achieves 7-fold sensitivity improvement, compared to a typical 125-μm FBG [13]. We obtain a downsized FBG with diameter of 60 μm after etching an FBG with a length of 10 mm for 1 hr with hydrogen fluoride (concentration 25%). The etched FBG is then coated with azobenzene-containing UV-curing resin of thickness 2 mm and length 40 mm. The synthesis method for the functional-coating material is discussed in deeper detail in reference [13]. The FBG has a center wavelength of 1546.2 nm and a spectral width of 0.15 nm, as seen in Fig. 5(a). Both the wavelength and spectral width are unchanged after the etching of the grating, as in Fig. 5(b). When the effective refractive index is assumed to be 1.45, the grating period can be determined to be 533.69 nm by the Bragg condition. When the etched FBG is subsequently coated with the polymer material, the center wavelength is shifted to 1545.62 nm, due to the fact that the polymer's shrinking during UV curing shortens the grating's spacing, as shown in Fig. 5(c). After that, the wavelength can recover to 1547.7 nm through UV exposure of the polymer-coated FBG, because the grating's period enlarges with UV-induced stretching of the coating material.

To control the shape of the reflection spectrum of the grating, the UV distribution on the grating can be easily changed by modifying the alignment between the centers of the UV LED and the grating. Here we also measure the group-delay response of the UV-induced chirped FBG, using an interferometry system combined with a Hilbert-transformation phase-retrieving algorithm [14]. The group-delay (GD) measurement for the CFBGs was conducted using a broadband light source and a simple fiber-optic Michelson-type interferometer. The interferogram of the reflection spectrum is obtained and the spectral phase ($\phi(\lambda)$) is calculated from the interferogram by use of the Hilbert-transformed interferogram, after high-pass filtering. The group delay τ_g and dispersion D can then be determined respectively by [1]

$$\tau_g(\lambda) = \frac{-\lambda^2}{2\pi c}\frac{d\phi}{d\lambda} \tag{6}$$

and

$$D = \frac{d\tau}{d\lambda}, \tag{7}$$

where c is the speed of light in vacuum. In the previous paper [9], we reported the spectral broadening of the UV-induced CFBG with the microactuator technique, but did not show any measurement of the GD profiles of the CFBGs.

Figure 6(a) shows the reflection spectral profile and its group delay for the UV-induced CFBG when the offset of the UV LED is +2.5 mm from the grating center. The abrupt spectral peak lies on the right side of the reflection spectrum, which means that the grating period is nonlinear at the end of the grating, as discussed in Section II. The

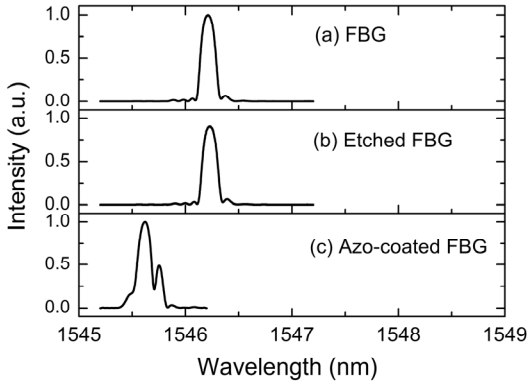

FIG. 5. Reflection intensities of (a) the FBG, (b) the etched FBG, and (c) the azobenzene-coated FBG.

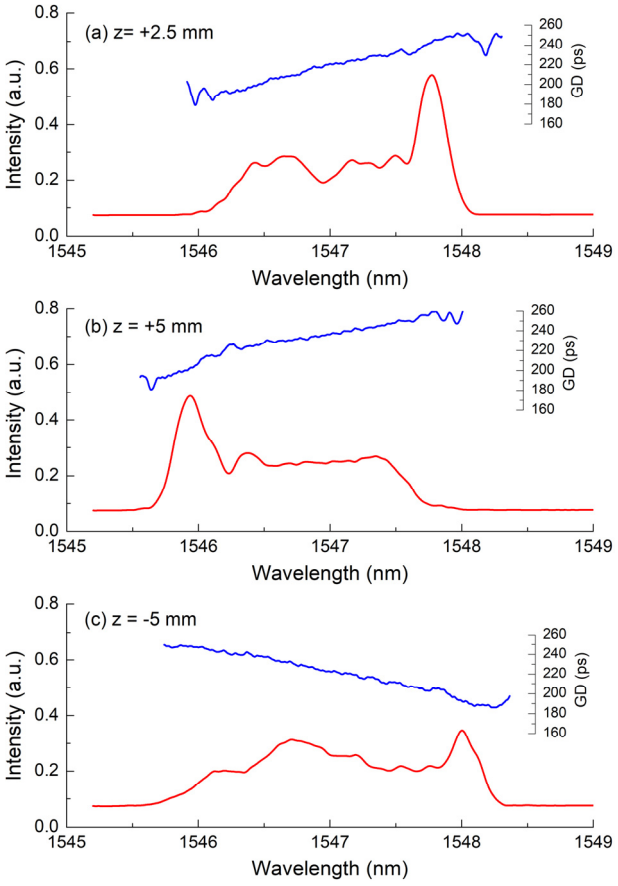

FIG. 6. The reflection spectra and group-delay (GD) profiles of a UV-induced CFBG, for LED displacements of (a) z = +2.5 mm, (b) z = +5 mm, and (c) z = -5 mm with respect to the grating's center.

spectrum agrees well with the simulated result of Fig. 2(b). The GD has a positive slope and is linear. The dispersion of the CFBG is determined to about 31.8 ps/nm for the spectral width of about 2 nm. Here we use the UV LED (LZ1-00UV0R, Engin Inc.) with a center wavelength of 365 nm and injection current to the LED of 0.38 A (applied voltage 3.6 V). The height of the LED above the grating is 1 cm; the full width at half maximum of the Gaussian-like UV beam from the LED is about 1.8 cm at a height of 1 cm.

The LED is subsequently moved to the offset position of +5 mm, which enables the FBG to have a nonlinear curve at the beginning of the grating, contrary to the case shown in Fig. 6(a). It is expected that the abrupt spectral peak now appears on the left side of the reflection spectrum, as shown in Fig. 6(b), according to the theoretical calculation. In this case the GD also has a positive slope, and the dispersion is determined to be about 27.6 ps/nm for the spectral width of 2 nm. The UV-induced dispersion of the CFBG decreases with increasing offset position, due to the fact that the light intensity also decreases toward the tail of the UV distribution. Alternatively, the dispersion can be increased at the same offset position by increasing the intensity of the UV LED, but in this case the center wavelength of the spectrum is also shifted simultaneously.

When we reverse the position of the LED, we can check whether the GD slope becomes negative. For the offset position of -5 mm, the reflection spectrum and GD profile are shown in Fig. 6(c). The GD switches to a negative slope and the dispersion is -25.68 ps/nm, as expected. The absolute dispersion value is nearly the same as that for the offset position of +5 mm in Fig. 6(b).

To obtain a flat-top reflection spectrum for the CFBG, we can control the intensity of the UV light, the misalignment of the center of the UV distribution with respect to the grating's center, and the height of the UV LED from the grating. Figure 7 shows the achieved flat-top reflection spectrum, in simulation and experiment. Here we set the LED's height to 1.5 cm, the displacement between the centers of LED and grating to 7.35 mm, and the LED injection current to 1.02 A (applied voltage 3.7 V), which results in a CFBG reflection response with spectral width of 1.38 nm and dispersion of 38.57 ps/nm, as shown in Fig. 7(b). In this case, we expect the FBG to lie in the most linear section of the Gaussian-like beam distribution from the UV LED. To check the prediction, we obtained the flat-top spectrum in a simulation (dashed curve in Fig. 7(b)) from the chirped grating spacing in Fig. 7(a) exposed to one side of the UV-intensity distribution. The flat-top spectrum from simulation is in good agreement with the actually measured reflection spectrum of the CFBG in Fig. 7(b).

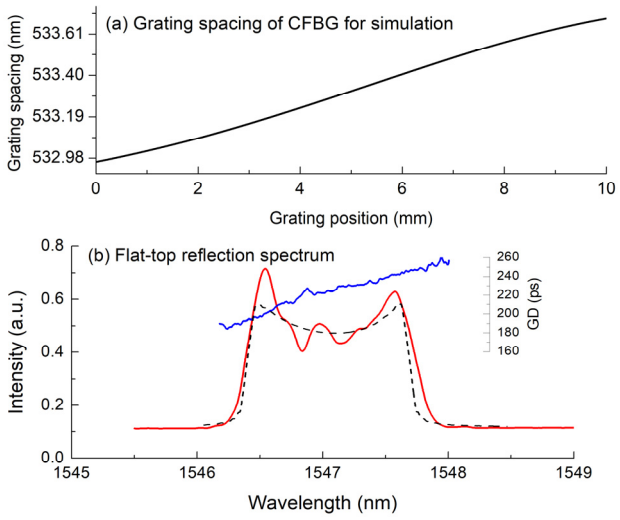

FIG. 7. Flat-top spectral shaping of the CFBG: (a) grating spacing for the flat-top spectrum in the simulation, (b) flat-top spectrum and GD profile of the CFBG in experiment (solid curves) and simulation (dashed curve).

IV. CONCLUSION

In this paper we have proposed a spectral-shape-controllable CFBG, achieved using a typical FBG with downsized diameter and coated with a UV-curable polymer containing a photomechanical material (the azobenzene moiety). The spectral shape of the CFBG can be controlled by adjusting the intensity profile from the UV LED by the height, displacement, and injection current of the LED. It is possible to obtain a special FBG with a nonlinear grating-period profile in combination with the polymer microactuator and UV LED. In addition, we found that the displacement direction of the LED enables one to switch the sign of the dispersion of the CFBG, from normal to anomalous dispersion. This spectral-shape-controllable CFBG device has great potential for use in tunable spectral filters, tunable pulse shapers, tunable dispersion compensators, and so on.

ACKNOWLEDGMENT

This study was supported by research funding from Chosun University, 2019.

REFERENCES

1. A. Othonos and K. Kalli, *Fiber Bragg grating: Fundamentals and Applications in Telecommunications and Sensing* (Artech House Print on Demand, MA, USA, 1999).
2. G.-S. Seo and T.-J. Ahn, "Protection method for diameter-downsized fiber Bragg gratings for highly sensitive ultraviolet light sensors," Curr. Opt. Photon. **2**, 221-225 (2018).
3. R. Kashyap, "Chirped fibre Bragg gratings for WDM applications," in Optical Amplifiers and Their Applications (Optical Society of America, 1997), paper FAW12.
4. D. Tosi, "Review of chirped fiber Bragg grating (CFBG)

fiber-optic sensors and their applications," Sensors **18**, 2147 (2018).
5. M. Buric, J. Falk, K. P. Chen, L. Cashdollar, and A. Elyamani, "Piezo-electric tunable fiber Bragg grating diode laser for chemical sensing using wavelength modulation spectroscopy," Opt. Express **14**, 2178-2183 (2006).
6. H. A. Fayed, M. Mahmoud, A. K. A. Seoud, and M. H. Aly, "Magnetically tunable fiber Bragg grating supported by guiding mechanism system," Proc. SPIE **7750**, 77501Z (2010).
7. Z. Li, V. K. S. Hsiao, Z. Chen, J. Y. Tang, F. L. Zhao, and H. Z. Wang, "Optically tunable fiber Bragg grating," IEEE Photon. Technol. Lett. **22**, 1123-1125 (2010).
8. Z. Li, Z. Chen, V. K. S. Hsiao, J.-Y. Tang, F. Zhao, and S.-J. Jiang, "Optically tunable chirped fiber Bragg grating," Opt. Express **20**, 10827-10832 (2012).
9. T.-J. Ahn and S. Moon, "Optically tunable fiber Bragg grating based on a photo-mechanical tuning mechanism," Opt. Lett. **44**, 2546-2549 (2019).
10. E. W.-G. Diau, "A new trans-to-cis photoisomerization mechanism of azobenzene on the $S_1(n, \pi^*)$ Surface," J. Phys. Chem. A. **108**, 950-956 (2004).
11. K. G. Yager and C. J. Barrett, "Azobenzene polymers as photomechanical and multifunctional smart materials," in *Intelligent Materials*, M. Shahinpoor and H.-J. Schneider, eds. (Royal Society of Chemistry, UK, 2008), Chapter 17.
12. I.-S. Song, W.-Y. Kim, C.-Y. Kim, B. H. Kim, H.-K. Kim, and T.-J. Ahn, "Sensitivity enhancement of a UV photo-sensor based on a fiber Bragg grating coated by a photo-mechanical functional polymer," Sens. Act. A **232**, 223-228 (2015).
13. G.-S. Seo, H.-T. Cho, O.-R. Lim, and T.-J. Ahn, "Highly sensitive and fact UV sensor based on fiber grating with easily producible photoreactive material," Sens. Act. A **283**, 169-173 (2018).
14. Y. Park, T.-J. Ahn, J.-C. Kieffer, and J. Azaña, "Optical frequency domain reflectometry based on real-time fourier transformation," Opt. Express **15**, 4597-4616 (2007).